A Spontaneous Water-Detaching Hydrophobic Coating Resistant to Calendar Aging Based on Non-Equilibrium Wetting

Jiaxue Yu‡, Wenting Wang‡, Yifan Li, Zilin Ye, Qiuhong Zhang, and Xudong Jia**

State Key Laboratory of Coordination Chemistry, Key Laboratory of High-Performance Polymer Material and Technology of MOE, Department of Polymer Science and Engineering, School of Chemistry and Chemical Engineering

Nanjing University

Jiangsu 210023, P. R. China

This PDF file includes:

Figs. S1 to S19

Tables S1 to S3

Legends for movies S1 to S8

Other Supplementary Materials for this manuscript include the following:

Movies S1 to S8

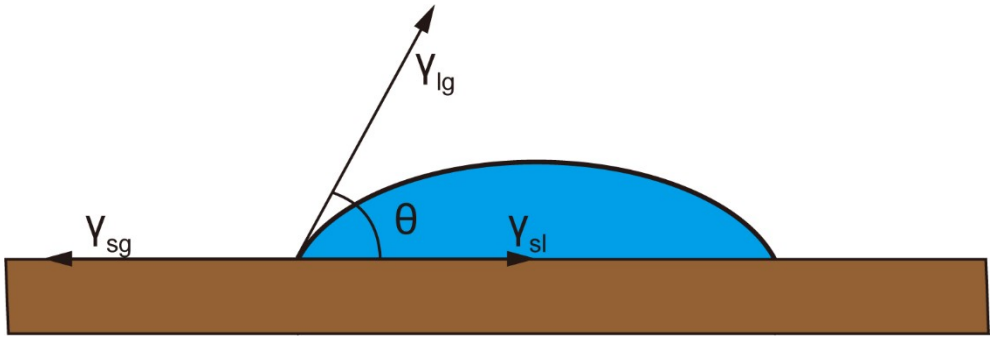

Fig. S1. Young's wetting model.
In equilibrium conditions, the contact angle is defined as the angle between the γ_{lg} and the γ_{sl}.

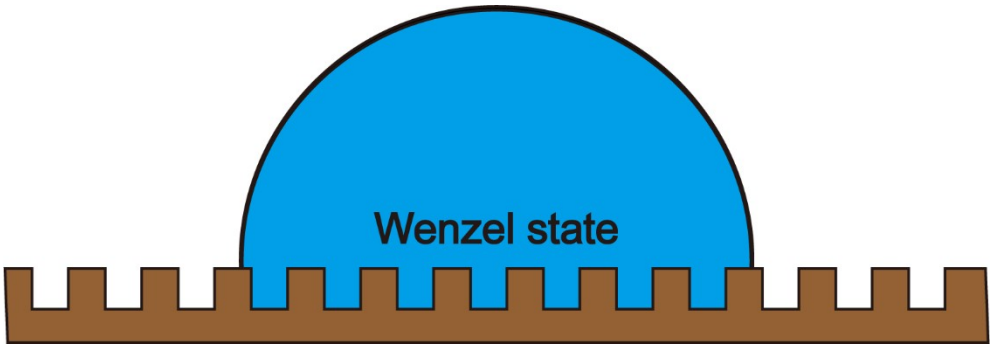

Fig. S2. Wenzel's wetting model.

To account for the discrepancy between the apparent and actual contact areas at the interface, the roughness factor (r) is introduced to modify the contact area.

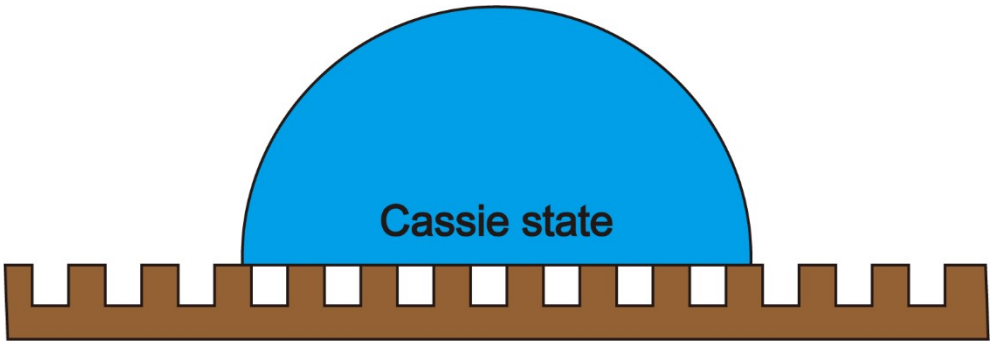

Fig. S3. Cassie's wetting model.

At the interface, the coexistence of gas and liquid phases and the contributions of the contact angles of individual phases to the apparent contact angle are considered.

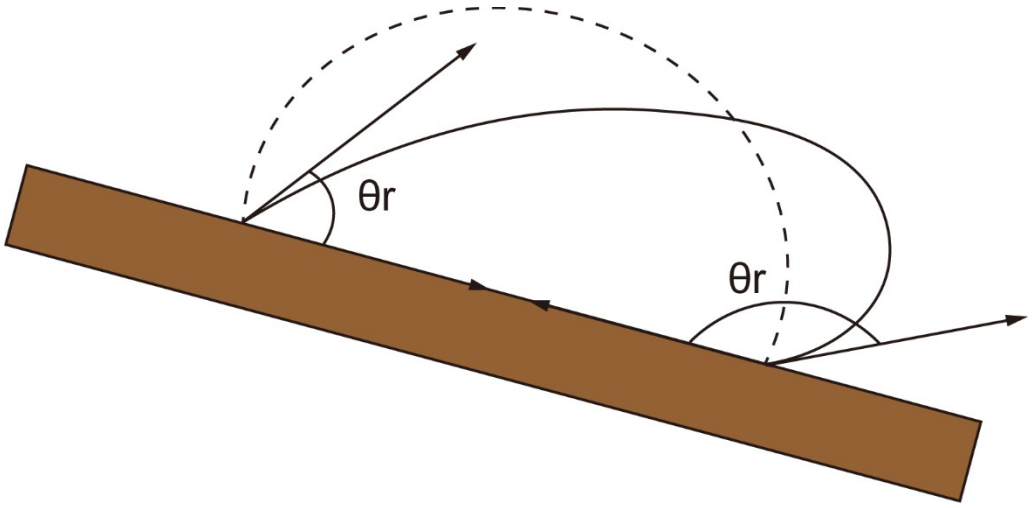

Fig. S4. A liquid droplet on an inclined hydrophobic surface exhibiting contact angle hysteresis.

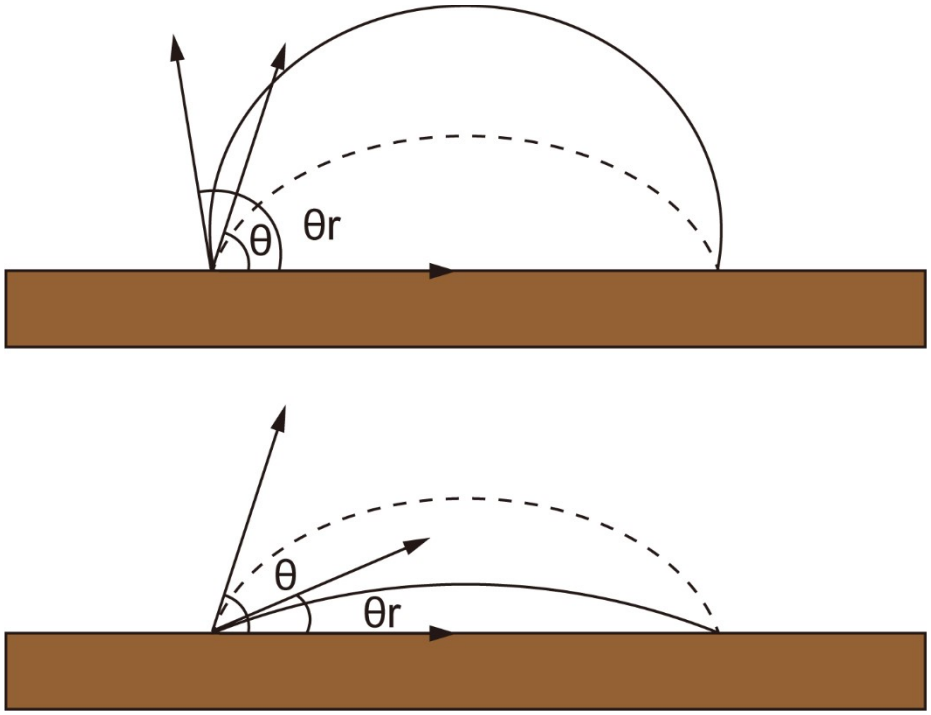

Fig. S5. A liquid droplet on a hydrophobic surface exhibiting contact angle hysteresis due to volume changes.

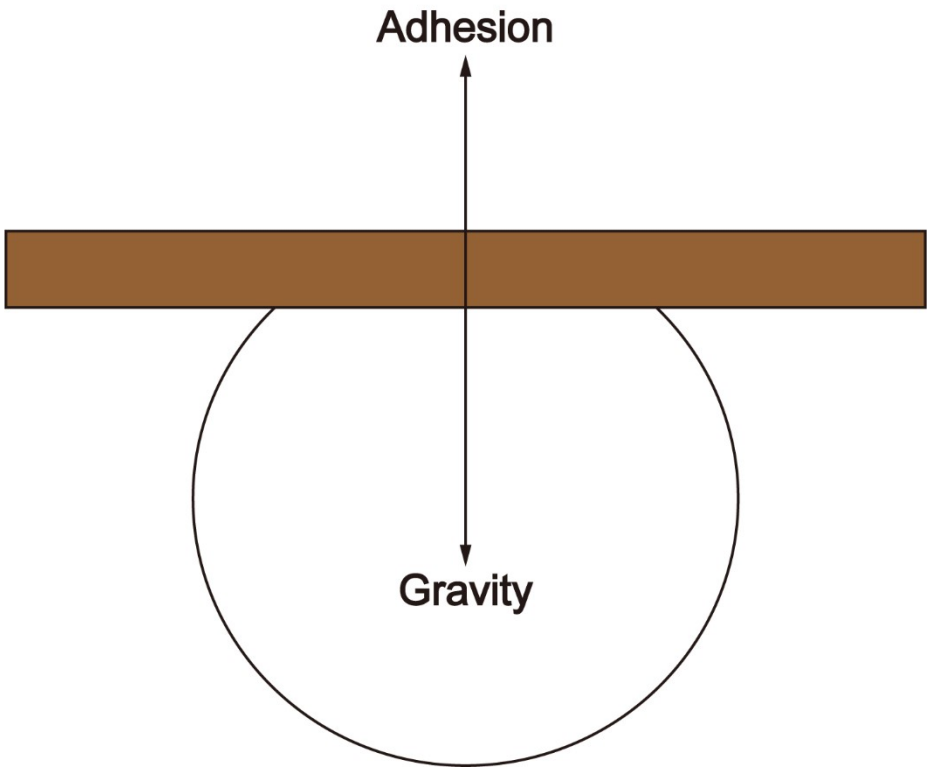

Fig. S6. A liquid droplet on a superhydrophobic surface experiencing an adhesion force equivalent to its own weight.

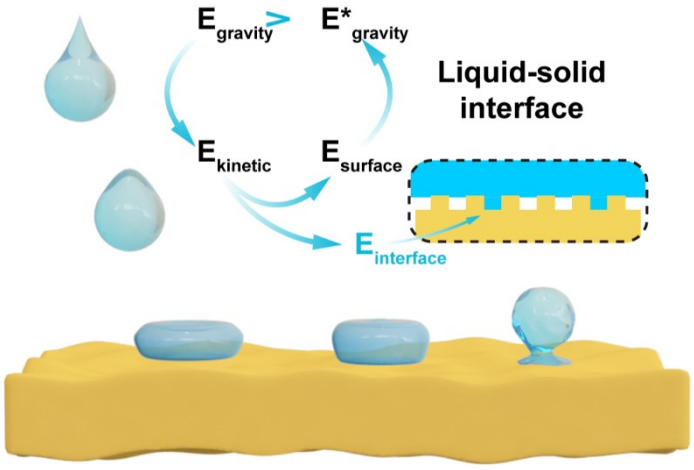

Fig. S7. Non-equilibrium wetting with interfacial energy generation.

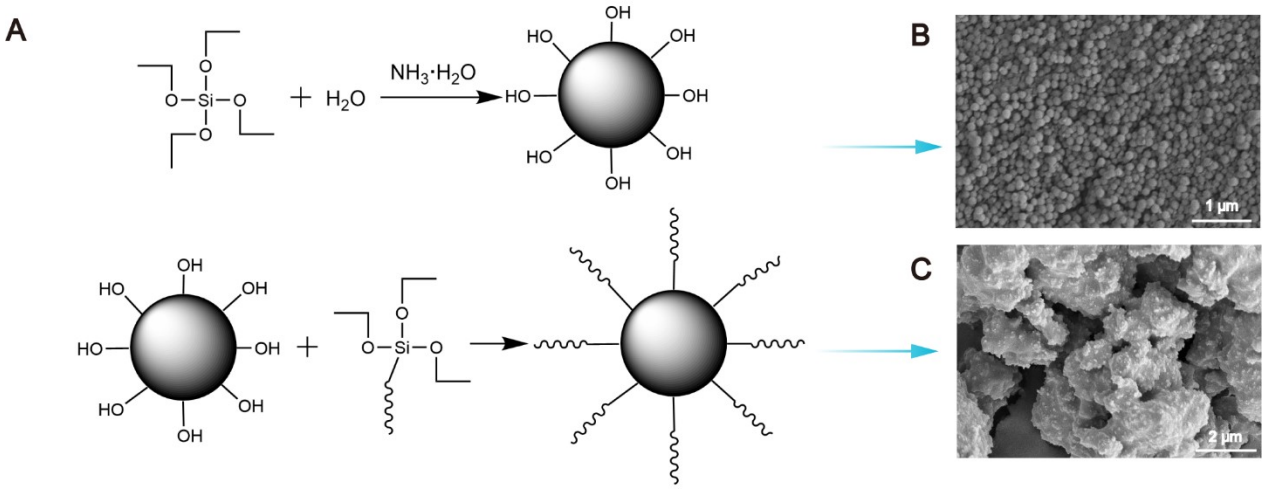

Fig. S8. Preparation of hydrophobic nanoparticles (HNP). (A) Schematic of the preparation of hydrophobic silica nanoparticles via the sol-gel method. **(B)** SEM image of nascent silica nanoparticles. **(C)** SEM image of hydrophobically modified silica nanoparticles.

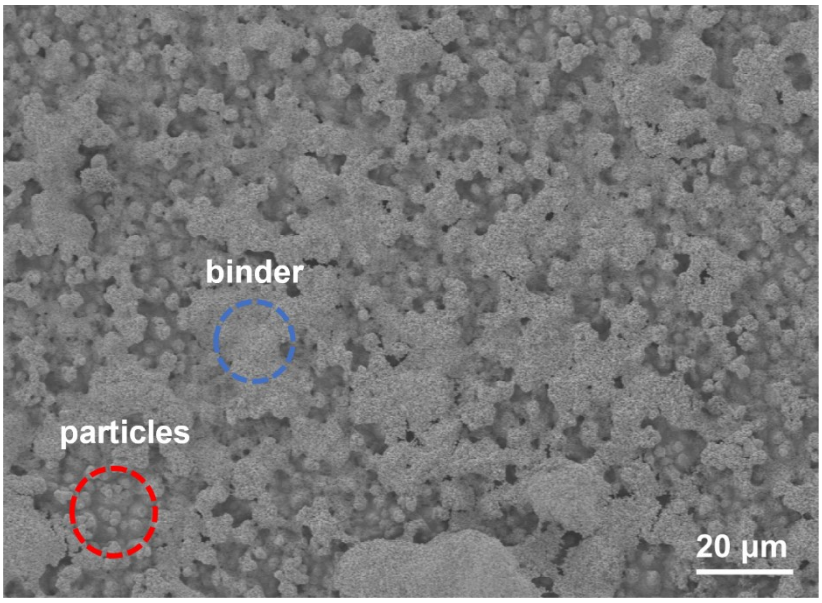

Fig. S9. SEM image of the HNP/SP composite coating prepared via high-speed mechanical dispersion.

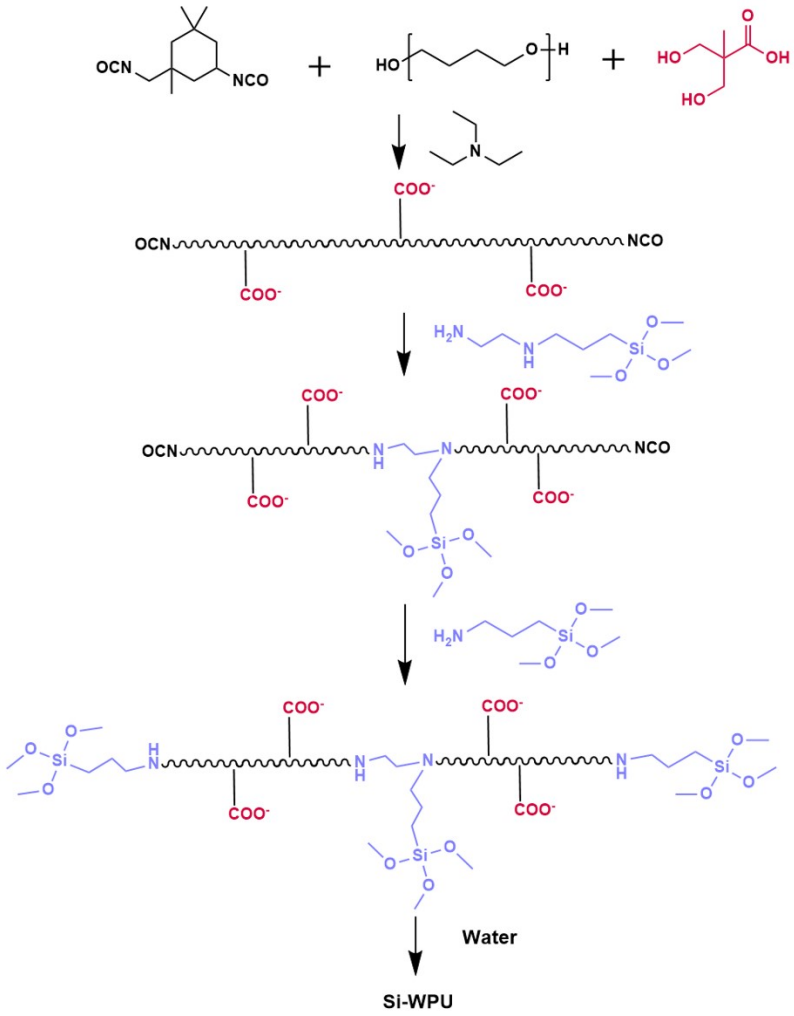

Fig. S10. Schematic of the preparation process of Si-WPU.

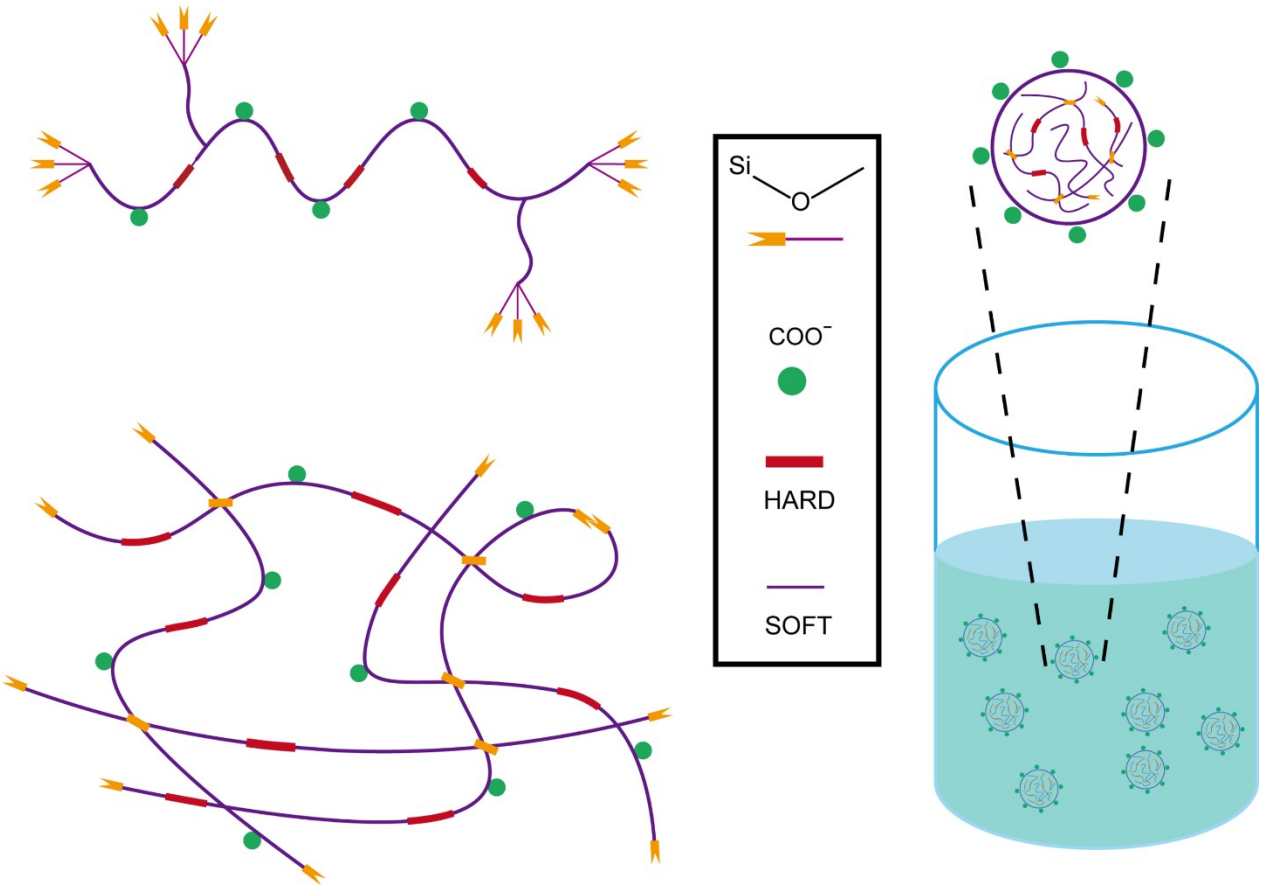

Fig. S11. Schematic diagram of the structure of Si-WPU emulsion.

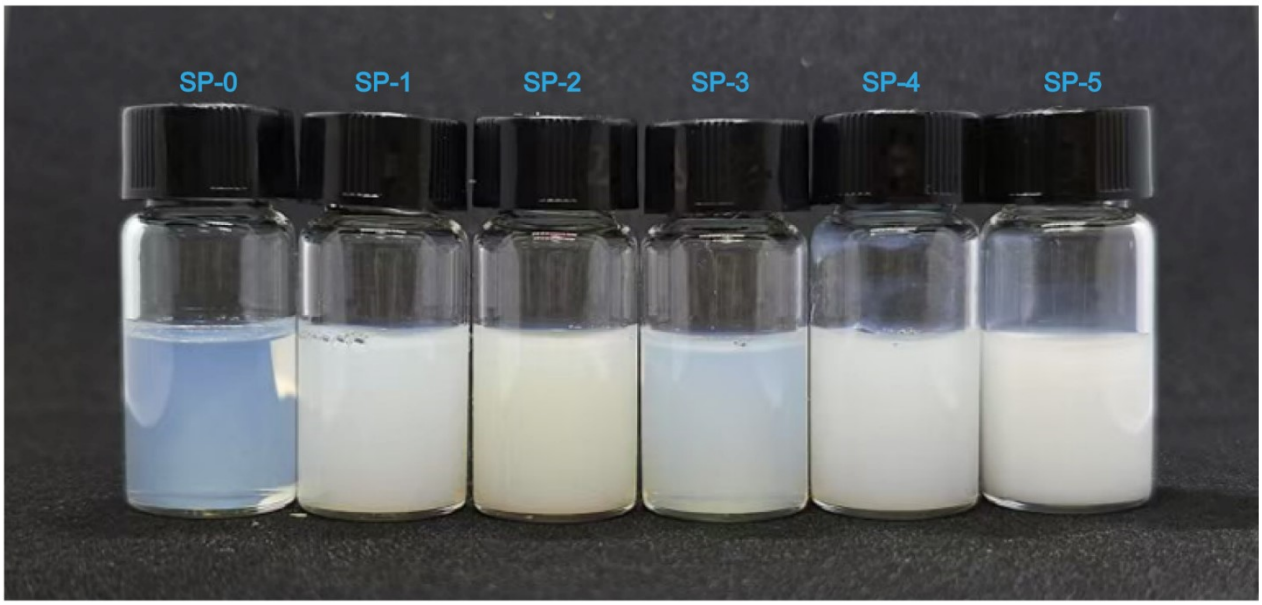

Fig. S12. Digital photographs of SP emulsions.

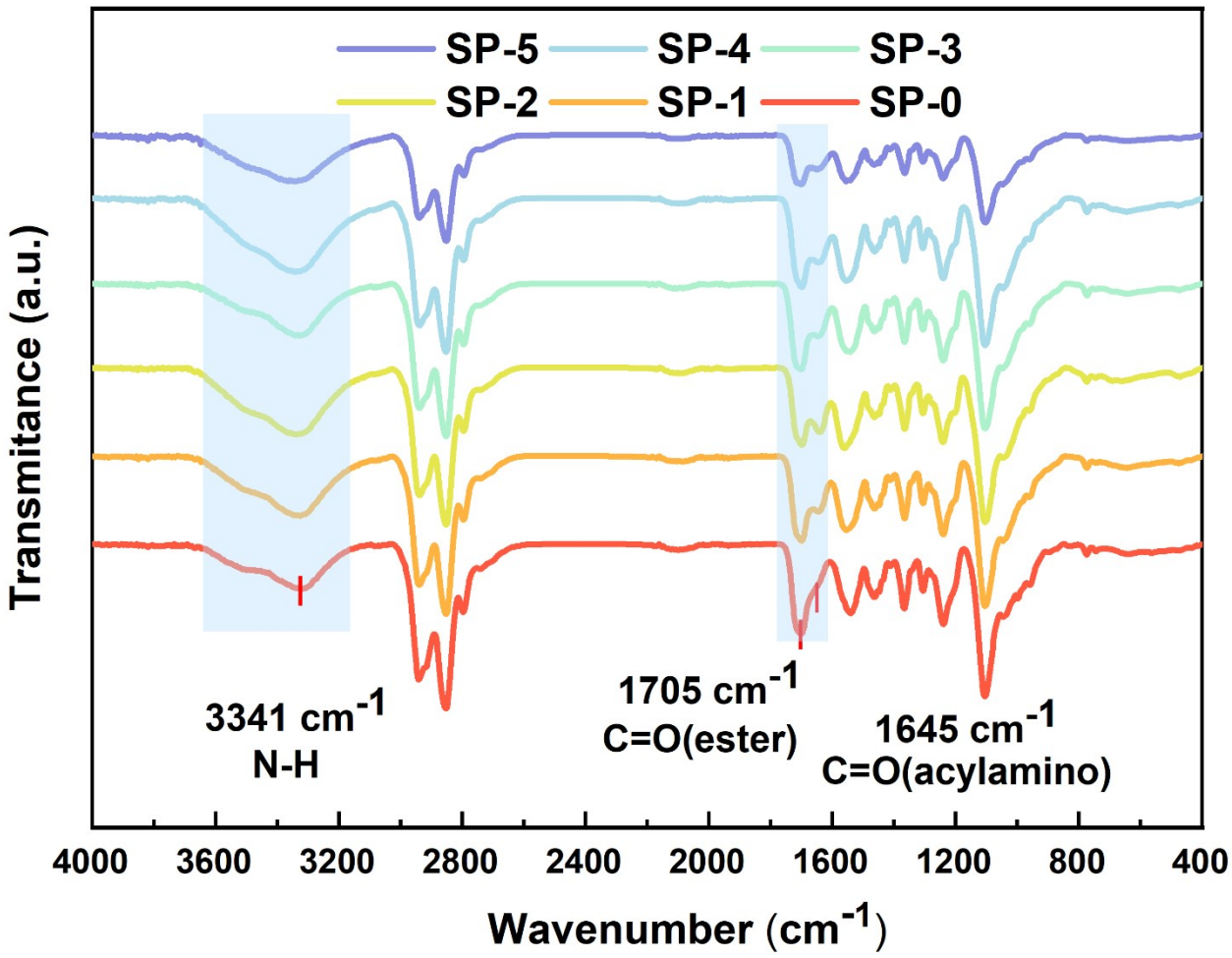

Fig. S13. Fourier-transform infrared spectra (FT-IR) of the SP films.

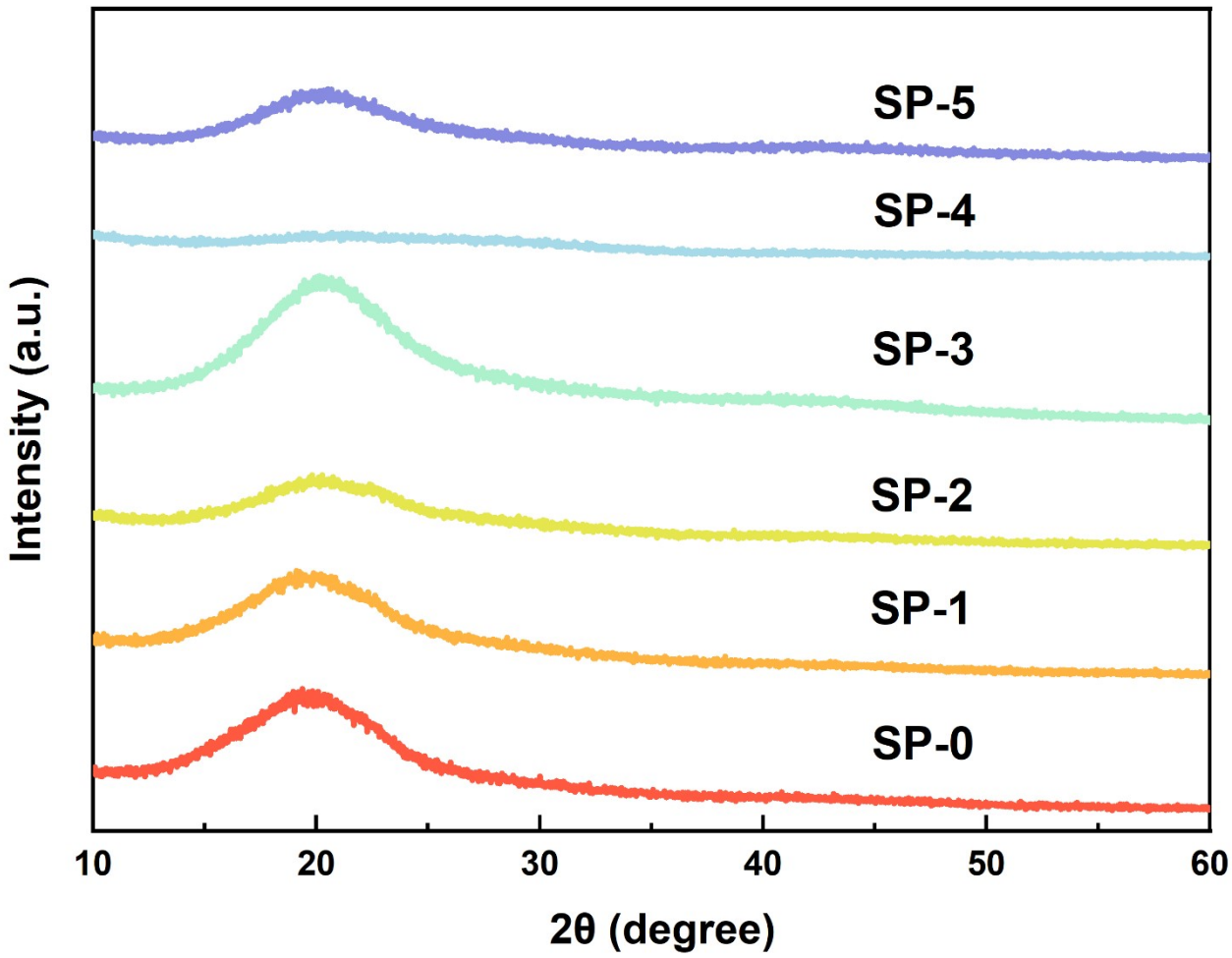

Fig. S14. Powder X-ray diffraction (PXRD) spectra of the SP films.

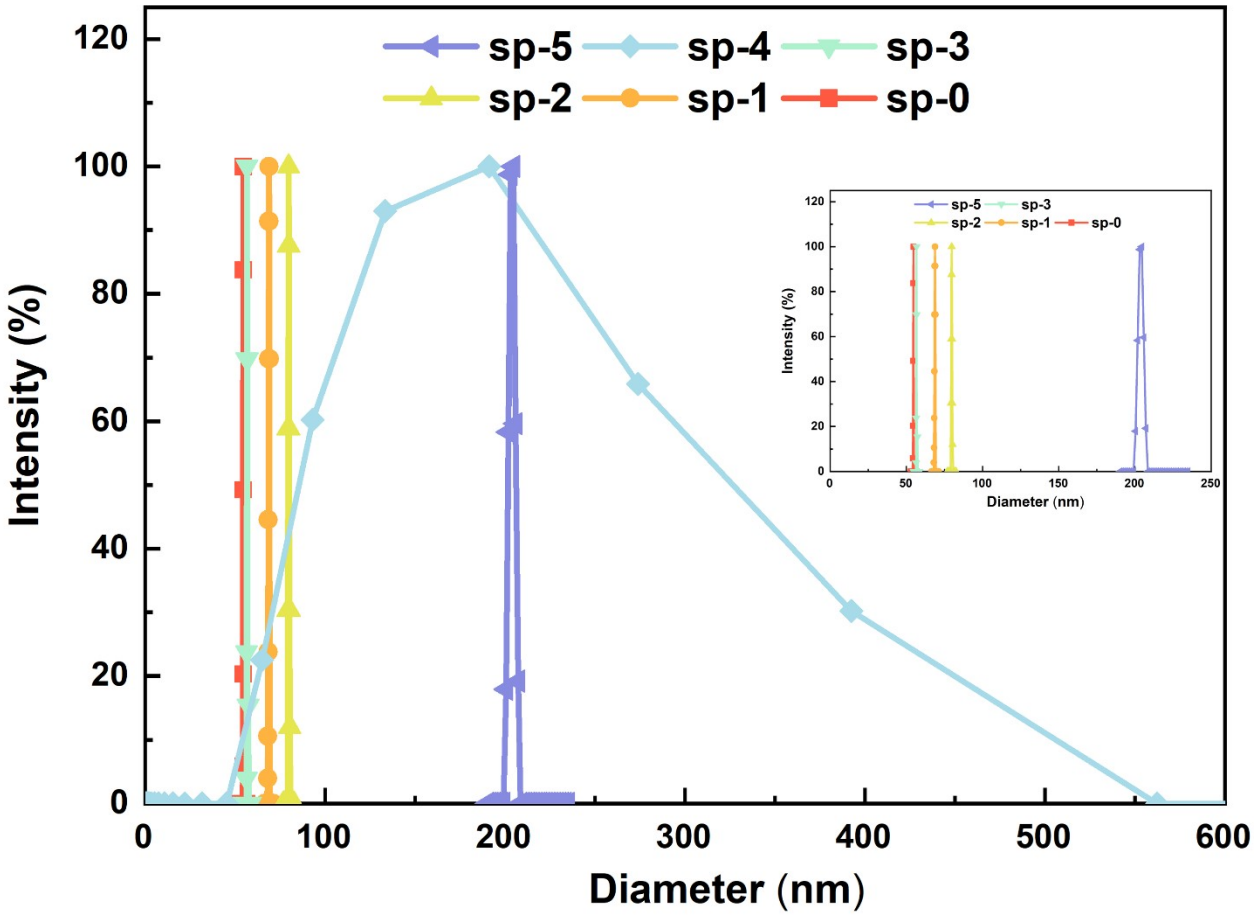

Fig. S15. Dynamic light scattering (DLS) spectra of the SP emulsions.

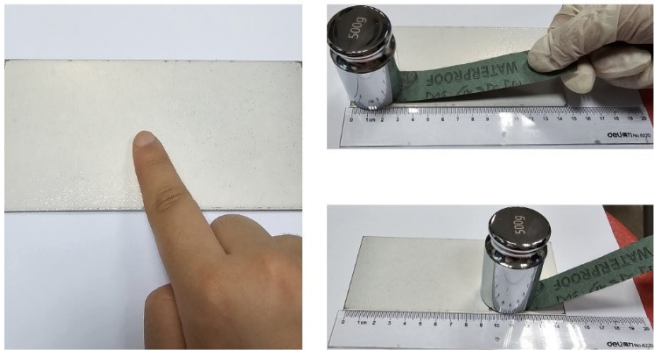

Fig. S16. Finger abrasion and sandpaper load abrasion tests of SP-5@HNP.

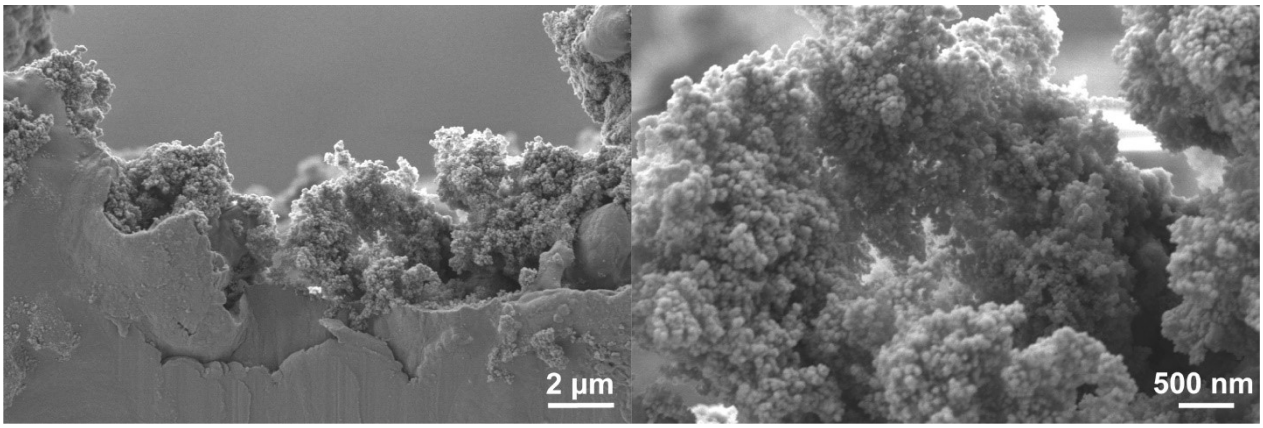

Fig. S17. Cross-sectional SEM images of SP-5@HNP coatings after friction testing.

Fig. S18. Caution signs for slippery surfaces are placed at Nanjing Metro XueZe Road station, and a dryer is used to remove water accumulation on the floor.

Fig. S19. Water repellency of SWDS-coated and SWDS-uncoated umbrellas. Hydrophobic coating with a thickness of approximately 1.5 μm was applied to the umbrella surface using a pneumatic spray gun, followed by complete curing at room temperature for 20 minutes.

Table S1. Material formulation of waterborne polyurethane emulsions.

Sample	Soft segment	Hard segment	Neutralizer	Chain extender 1	Chain extender 2	Blocking agent	R	Solid content
	PTMG-2k	IPDI	TEA	DMPA	AATS	ATS		
SP-0	9.50 g 4.75 mmol	3.36 g 15.1 mmol	0.60 g 6.00 mmol	0.75 g 6.00 mmol	/	/	2.00	26.58%
SP-1	9.50 g 4.75 mmol	3.36 g 15.1 mmol	0.60 g 6.00 mmol	0.75 g 6.00 mmol	/	1.11 g 5.00 mmol	1.70	27.46%
SP-2	9.50 g 4.75 mmol	3.36 g 15.1 mmol	0.60 g 6.00 mmol	0.75 g 6.00 mmol	/	2.21 g 10.0 mmol	1.50	26.92%
SP-3	9.50 g 4.75 mmol	3.36 g 15.1 mmol	0.60 g 6.00 mmol	0.75 g 6.00 mmol	0.20 g 1.75 mmol	1.11 g 5.00 mmol	1.56	27.05%
SP-4	9.50 g 4.75 mmol	3.36 g 15.1 mmol	0.60 g 6.00 mmol	0.75 g 6.00 mmol	0.39 g 3.50 mmol	1.11 g 5.00 mmol	1.42	27.37%
SP-5	9.50 g 4.75 mmol	3.36 g 15.1 mmol	0.60 g 6.00 mmol	0.75 g 6.00 mmol	0.39 g 3.50 mmol	0.55 g 5.00 mmol	1.52	26.83%

Table S2. Interaction energy between Si-O-C side group and solvent (Ha)

Solvent	Distance/ Å				
	5	4.5	4	3.5	3
Water	-824.65795	-824.657769	-824.657963	-824.657645	-824.652002
Ethanol	-902.53347	-902.534973	-902.536478	-902.530622	-902.480444

Table S3. Long-term hydrophobic performance of SWDS under various climatic conditions across China.

City	Beijing	Anshan	Qingdao	Taiyuan	Xi'ning	Chengdu	Dongguan	Hefei	Suzhou	Wuxi
Precipitation/mm	400-600	800-1200	800-1200	400-600	200-400	600-800	1600-2000	600-800	1200-1600	1200-1600
Month	11	9	11	10	7	10	13	14	18	12
Water Adhesion Ratio/%	0.6	0.2	0.5	0.7	1.2	0.8	0.2	0.4	0.2	0.4

Movie captions:

Movie S1. Non-equilibrium wetting behavior of low-velocity water droplets on the SP-0@HNP.

Movie S2. Non-equilibrium wetting behavior of low-velocity water droplets on the SP-1@HNP.

Movie S3. Non-equilibrium wetting behavior of low-velocity water droplets on the SP-2@HNP.

Movie S4. Non-equilibrium wetting behavior of low-velocity water droplets on the SP-3@HNP.

Movie S5. Non-equilibrium wetting behavior of low-velocity water droplets on the SP-4@HNP.

Movie S6. Non-equilibrium wetting behavior of low-velocity water droplets on the SP-5@HNP.

Movie S7. Non-equilibrium wetting behavior of high-velocity water droplets on the SWDS after abrasion testing.

Movie S8. Hydrophobicity of SWDS after 18 months of outdoor exposure.